



Neuromelanin-sensitive MRI of the substantia nigra: An imaging biomarker to differentiate essential tremor from tremor-dominant Parkinson's disease

Jian Wang^{b,c,1}, Zhen Huang^{a,1}, Yuanfang Li^{a,1}, Fang Ye^{b,c}, Changpeng Wang^a, Yong Zhang^d, Xiaoqin Cheng^a, Guoqiang Fei^a, Kai Liu^{b,c}, Mengsu Zeng^{b,c}, Chunjiu Zhong^a, Lirong Jin^{a,*}

^a Department of Neurology, Zhongshan Hospital, Fudan University, China

^b Department of Radiology, Zhongshan Hospital, Fudan University, China

^c Shanghai Medical Imaging Institute, Shanghai, China

^d MR Research, GE Healthcare, Shanghai, China

ARTICLE INFO

Keywords:

Parkinson's disease
Essential tremor
Neuromelanin
Magnetic resonance imaging
Diagnostic test

ABSTRACT

Introduction: We aimed to evaluate whether neuromelanin-sensitive MRI (NM-MRI) features in the substantia nigra pars compacta (SNc) were of diagnostic value to differentiate untreated essential tremor (ET) from *de novo* tremor-dominant Parkinson's disease (PD_T).

Methods: Eighteen untreated ET patients, 21 *de novo* PD_T patients and 21 healthy control subjects were recruited. All the subjects underwent clinical examination, motor and cognitive evaluations, as well as NM-MRI. High signal intensity of the lateral, central and medial SNc subregions on NM-MRI were evaluated using the width, signal intensity (contrast-to-noise ratio, CNR) and visual analysis. Diagnostic test performance of SNc values was investigated by using receiver operating characteristic analysis and net reclassification improvement (NRI).

Results: The width and CNR values of the lateral and central SNc subregions in PD_T were significantly decreased compared with those in ET and control group. Using visual analysis, the total visual score of all SNc subregions was significantly reduced in PD_T when compared with ET and control group. The width of the lateral SNc subregion allowed the best differentiation between ET and PD_T, and visual analysis also showed good diagnostic value. NRI result indicated that visual analysis and the width of the lateral SNc subregion had the same diagnostic power.

Conclusions: The neuromelanin changes of SNc in ET and PD_T follow the different patterns. Both the measurements and visual analysis of SNc on NM-MRI provide high diagnostic accuracy for differentiating ET from PD_T subtype. NM-MRI is a potential tool in diagnostic work-up of tremor disorders.

1. Introduction

Essential tremor (ET) is the most common motor disorder in the elderly [1], with a characteristic motor feature as a symmetric 4–8 Hz action tremor that most frequently affects the hands and arms. However, it remains a challenge to differentiate ET from tremor-dominant Parkinson's disease (PD_T) in the early stage [2], considering the complex clinical manifestations, for example, more than 48% of patients with Parkinson's disease (PD) have action tremor [3] while 18% of patients with ET experience resting tremor [4]. Jain S reported that approximately one-third of the ET patients were misdiagnosed as the other motor disorders, especially of PD_T and dystonia [5]. Therefore, it is of significant clinical value to find a new biomarker for better

distinguishing ET from the early stage PD tremor dominant subtype.

On the other hand, the etiology and pathophysiology of ET are still little to be known. In recent years, more and more clinical and pathological evidence has been found that ET might be a neurodegenerative disorder and have a relationship with PD [6,7]. For example, patients with ET have non-motor features, such as cognitive abnormalities characterized by mild frontal dysfunction, anxiety, depression, and olfactory dysfunction, etc [8]. Moreover, pathologically degenerative changes were also found in the brains of ET patients in a postmortem study [9], despite another study obtained no significant basis of cerebellar purkinje cell loss in ET [10]. As we know, neuroimaging is an important alternative approach to understand the pathological basis and nerve loop of ET in vivo, considering few patients could receive a

* Corresponding author.

E-mail address: jinlr99@163.com (L. Jin).

¹ Co-first authors.

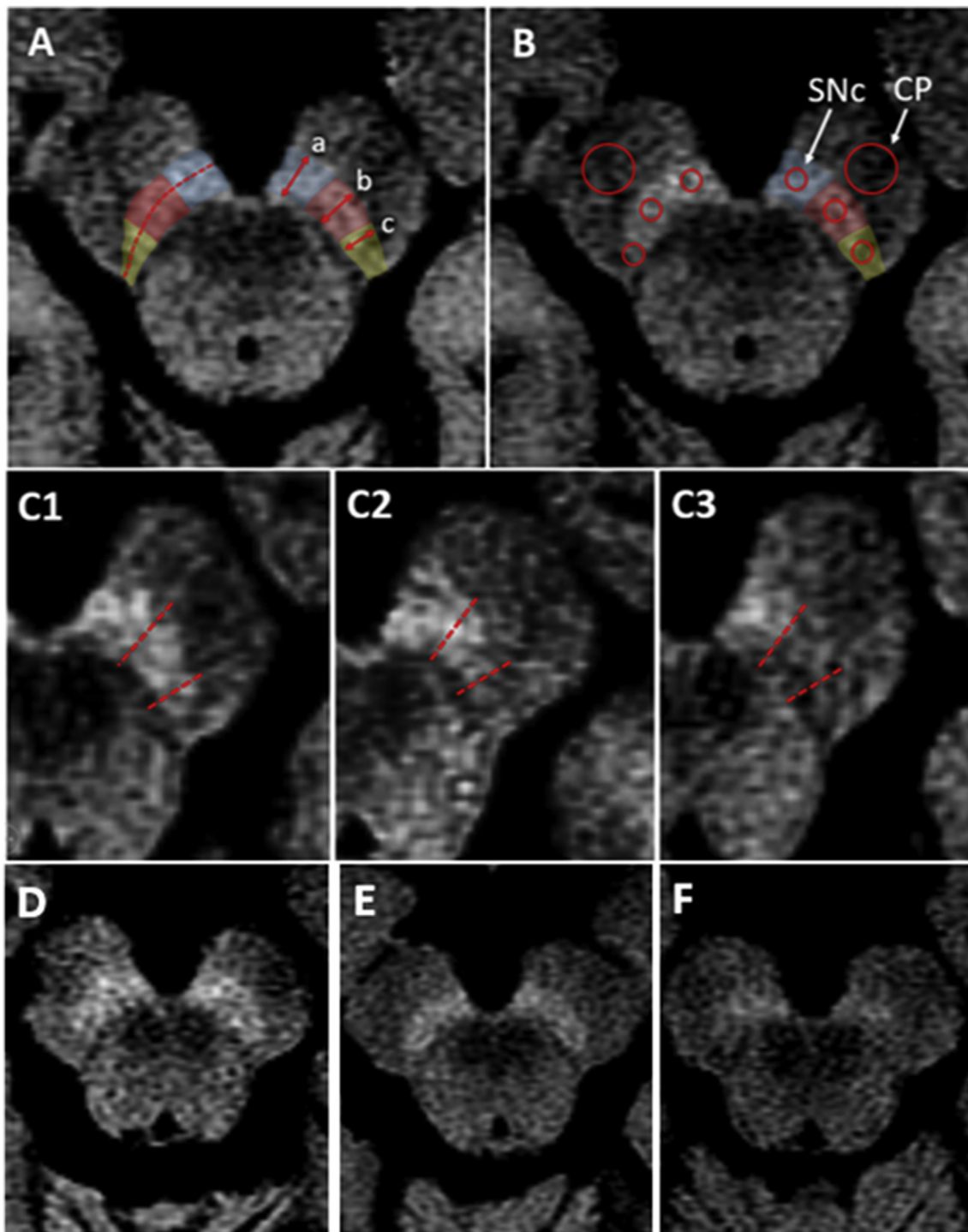


Fig. 1. (A) Division and width measurement of SNc. Blue, red and yellow areas represented medial, central, and lateral subregions respectively. The dotted line indicated the longitudinal length line of SNc. Widths of medial, central, and lateral SNc subregions were indicated by the double arrows labeled with a, b and c. (B) Signal intensity measurement of SNc. (C) Visual assessment. Take the central subregion for example, C1, C2 and C3 represented score 2, 1 and 0 respectively. (D) Control (E) ET patient (F) PD_T patient. (For interpretation of the references to colour in this figure legend, the reader is referred to the Web version of this article.)

postmortem examination for ET. Previous neuroimaging studies have demonstrated the changes of the substantia nigra (SN) in ET patients such as increased echogenicity in sonography studies [11] as well as reduction of MRI T2*-relaxometry signal [12], which suggested that ET is associated with brain iron deposition. However, another neuroimaging study, a three-year follow up study with DAT-SPECT, found no decline of DAT binding in ET patients, which was against the neurodegeneration hypothesis of ET [13]. Thus, the conflicting results

emphasize the need to make further studies between ET and PD.

In the substantia nigra pars compacta (SNc), neuromelanin is the main way to store iron and to prevent the generation of superoxide free radicals against iron-mediated neurotoxicity [14]. T1-weighted neuromelanin-sensitive magnetic resonance imaging (NM-MRI) can reflect the changes of neuromelanin [15]. So far, there was only one study that using NM-MRI to focus on the disparity between ET and PD, and its results demonstrated that neuromelanin in the SNc was markedly

decreased in the PD group when compared with the ET and control groups [16]. However, the study was subject to the small sample size thus not to compare the difference in neuromelanin changes on NM-MRI between ET patients and PD clinical subtypes, particularly tremor-dominant PD patients, yet ET and PD_T have some overlaps in clinical manifestations that make it difficult to differentiate them from each other.

In this study, we aimed to evaluate whether NM-MRI features in SNc was of diagnostic value to differentiate untreated patients with ET from those with *de novo* PD_T.

2. Subjects and methods

This study was approved by the Committee on Medical Ethics at Zhongshan Hospital, Fudan University and informed consent was obtained from each subject.

2.1. Study subjects

Eighteen patients with untreated ET, 21 patients with *de novo* PD_T, and 21 healthy control subjects were voluntarily recruited from September 2016 to August 2017. ET patients were diagnosed according to the criteria of the Consensus Statement of the Movement Disorders Society on Tremor [17]. PD patients were diagnosed according to the criteria of the MDS clinical diagnostic criteria for Parkinson's disease [18], meanwhile the subgroup of primarily tremor with minimal bradykinesia and rigidity was fitted into tremor-dominant PD according to UPDRS III score, as previously reported [19]. All the patients were drug naïve. The exclusion criteria included a history of other neurological/psychiatric disorders, abnormal signal that affected further analysis on structural MR imaging, severe infection, liver dysfunction, renal insufficiency, past/current substance abuse, and tremor related dysmetabolism including thyroid dysfunction and drug toxicity. Control subjects had no history of head trauma, stroke, or other neuropsychological diseases and no first-degree relatives with ET or PD.

2.2. Magnetic resonance imaging acquisition

All the MR data was acquired on a 3-T MR unit (Discovery™ MR750, GE Healthcare, Milwaukee, WI). NM-MRI was performed using T1-weighted fast spin-echo sequence with the following parameters: TR/TE, 600/13 ms; echo train length, 2; section thickness, 2.5 mm, with no intersection gap; number of slices, 16; matrix size, 512 × 320; field of view (FOV), 220 mm; NEX, 5; and acquisition time, 8 min 3 s. The axial sections were scanned parallelly to the anterior commissure-posterior commissure line with a coverage from the posterior commissure to the pons. In addition, conventional MRI sequences were obtained and then evaluated by a ten-year experienced neuroradiologist (W.J.) to exclude other pathological imaging findings that might interfere with further assessment.

2.3. Imaging analysis

All the NM-MRI images were transferred to a commercial available workstation (ADW4.6, GE Healthcare) and were displayed in a certain setting (window width 400, window level 850–900) for analysis.

2.3.1. Quantitative measurements

One of the authors (W.J.) who was blinded to the subjects' information performed quantitative image analysis twice, with a time interval of at least 7 days. The middle slice with the greatest SNc area in the three consecutive slices in which SNc high signal was visible, was selected for measurements. In the selected slice, the maximal longitudinal length line of SNc was divided into three equal segments to define the lateral, central, and medial subregions of SNc (Fig. 1 A) [16]. The maximal width of the high signal intensity perpendicular to the

longitudinal length line in each SNc subregion (Fig. 1 A) was measured. A maximal width of zero means that the corresponding SNc subregion was invisible. Circular regions-of-interest (ROIs) were placed in the center of SNc subregions and the adjacent cerebral peduncles (CP). The mean signal intensity (SI) and standard deviation (SD) in the ROIs were recorded. The ROI size was 2 mm² for SNc subregion, and 10 mm² for CP (Fig. 1 B). The contrast-to-noise ratio (CNR) between SNc and CP was calculated using the following equation: $CNR_{SNc} = (SI_{SNc} - SI_{CP}) / SD_{CP}$. SI_{SNc} represented the SI of SNc subregion. SI_{CP} and SD_{CP} in the equation represented the mean SI and mean SD of bilateral CP, respectively. As no significant differences were found in the measured widths and CNRs of the SNc subregions between the left and right sides, the values were obtained from an average of both SNc sides. Then, the mean value of the twice measurements was used for statistical analysis.

2.3.2. Visual analysis

Two radiologists (a ten-year experienced neuroradiologist W.J. and a general radiologist Y.F.) who were blinded to the subjects' information performed visual analysis of SNc high signal on NM-MRI, independently. The neuromelanin high signal shown in each subregion was rated on an ordinal scale with 3 increments: 2, definitely or probably visible integrally in the subregion; 1, possibly or partly visible in the subregion; 0, probably or definitely invisible in the subregion (Fig. 1 C1-3). If disagreement arose between their ratings, they consulted to reach a consensus. Afterwards, a sum of all SNc subregions' scores obtained from their consensus was calculated as the total visual score (from 0 to 12) for statistical analysis.

2.4. Statistical analysis

All continuous values were expressed as mean ± standard deviation (SD). For demographic and clinical characteristics, we used one way ANOVA and independent *t*-test to compare the quantitative predictors among and between groups, while the chi-square test to compare categorical predictors among groups. One way ANOVA analysis was used to compare the SNc quantitative parameters including widths and CNRs among groups, with Scheffe or Games-Howell test (depending on the homogeneity of variance) for post hoc comparisons. Kruskal-Wallis test was used to compare the SNc total visual scores. Intra-observer agreement of quantitative measurements was determined by calculating the intra-class correlation coefficient (ICC), while inter-observer agreement of visual scores in each subregion was determined using kappa test. A receiver operating characteristic (ROC) analysis was performed to determine which NM-MRI parameters discriminated PD_T group and ET group. Net reclassification improvement (NRI) was used to compare the total visual score and a quantitative biomarker with the best diagnostic power in all NM-MRI quantitative parameters [20]. A value of *p* < 0.05 was considered as a statistical significant difference. All statistical tests were performed using the SPSS (Statistical Package for the Social Sciences) statistical software package (SPSS for Windows, version 18.0; Chicago, IL).

3. Results

3.1. Demographic and clinical data

Demographical and clinical characteristics of patients and healthy controls were summarized in [Esupp files Table1](#). There was no significant difference among ET, PD_T and control subjects in age, gender, MoCA score, and MMSE score. Disease durations in ET group were significantly longer than those in PD_T group (9.97 ± 8.04 vs 1.72 ± 1.56 , *p* < 0.001), and UPDRS tremor score in ET group were significantly lower than PD_T group (2.33 ± 1.46 vs 3.52 ± 1.66 , *p* = 0.024). In ET group, involvement of tremors was present bilaterally in all patients (100%), despite 7 individuals (38.9%) presented slightly asymmetrical tremors. In addition, there were 18 ET patients (100%)

with postural tremors, 12 (66.7%) with kinetic tremors, 1(5.6%) with head tremors, 1(5.6%) with voice tremors, none (0%) with rest tremors or dystonic features, and 14 patients (77.8%) with a family history of ET. In *de novo* PD_T group, patients had mild disease severity with Hoehn and Yahr stages from 1 to 2.

3.2. Quantitative measurements and visual analysis of SNc

Intra-observer agreement (W.J.) was good to excellent for widths and CNRs of all SNc subregions: ICC was ranged from 0.686 to 0.896 for width, and from 0.750 to 0.919 for CNR. The Kappa values of visual rating analysis in SNc subregions between two observers (W.J. and Y.F.) were ranged from 0.364 to 0.736 which indicated moderate consistence of visual analysis in most subregions. Furthermore, ICC value of inter-observer agreement (W.J. and Y.F.) was 0.814 when the repeatability of total visual scores was evaluated, which indicated the high consistence of the total visual score between two radiologists (See [Esupp files Table 2](#) for more details).

One-way ANOVA analysis showed that the widths of the central and lateral SNc subregions presented significant difference among PD_T, ET and control groups ($p < 0.001$, [Esupp files Table 3](#)). Using *post hoc* Games-Howell test for further comparison, the widths of the central and lateral SNc in PD_T patients were significantly decreased compared to those in ET and control groups ($p < 0.01$, [Fig. 1 D–F](#), [Fig. 2A](#)). Similarly, the CNRs of the central and lateral subregions had significant difference among the three groups ($p < 0.001$ for the central

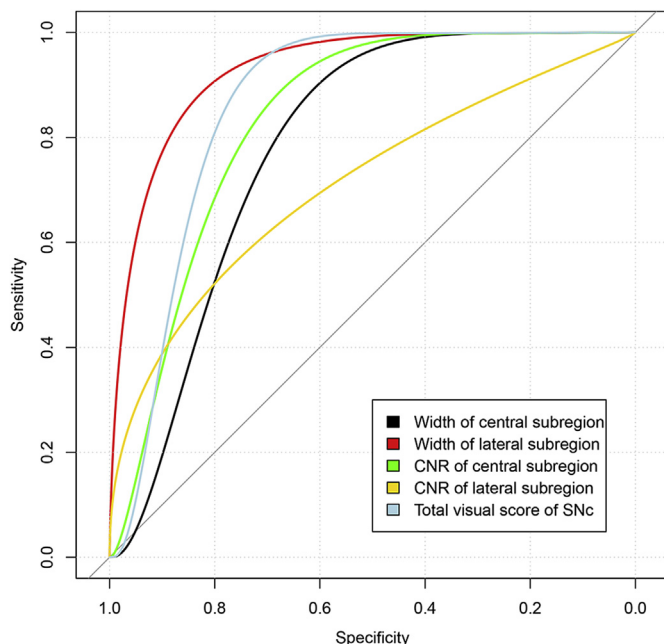


Fig. 3. ROC analysis of NM-MRI for differentiating ET from PD_T patients.

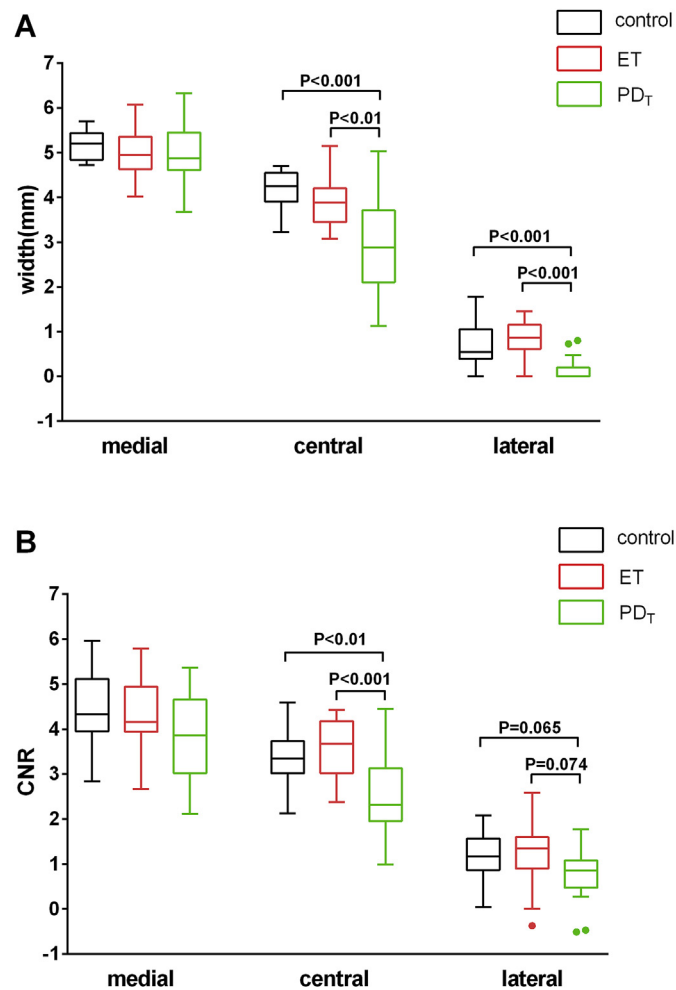


Fig. 2. Box plot illustrated subregional width (A) and contrast-to-noise ratio (B) of SNc neuromelanin high signal in patients with ET, *de novo* PD_T and control subjects.

subregion and $p = 0.029$ for the lateral subregion, respectively. [Esupp files Table 3](#) and [Fig. 1D–F](#)). Then the Scheffe test was used for comparison between multiple groups. The results had demonstrated that the CNR of the central SNc subregion was lower in the PD_T group than those in the ET ($p < 0.001$) and control groups ($p = 0.003$), while the CNR of lateral subregion in PD_T patients had a decreasing tendency, but not reaching significance (PD_T vs control, $p = 0.065$; PD_T vs ET, $p = 0.074$, [Fig. 2B](#)). There was no significant difference in the width or CNR of the medial SNc subregion among three groups. In addition, the width and CNR did not show significant difference in any SNc subregion between the ET and control groups ($p > 0.05$). We also found that the total visual scores of SNc on NM-MRI were significantly reduced in PD_T group compared with the ET and control groups ($p < 0.001$).

3.3. Diagnostic performance value of NM-MRI to differentiate ET from PD_T

On basis of the findings above, the widths of the central and lateral SNc subregions, the CNRs of central and lateral SNc subregions and the total visual score of SNc were used in the ROC curve to evaluate the diagnostic accuracy of NM-MRI. The result of ROC analysis was shown in [Fig. 3](#). The area under ROC curve(AUC) for discriminating ET from PD_T was the largest for the width of the lateral SNc subregion (0.923), followed by the CNR of central subregion (0.836), the width of central subregion (0.787), and the CNR of lateral subregion (0.728). The AUC value for the total visual score of SNc was 0.865, which also demonstrated good diagnostic value.

The sensitivity and specificity for differentiating the ET patients from PD_T patients were 90.5% and 83.3%, respectively, when the cutoff value for the width of lateral subregion was set as 0.525 mm. The optimal cut-off level for the total visual score of SNc that discriminated between ET and PD_T groups was 7.5. Since the scoring system did not include 0.5, it could be inferred that a score of ≥ 8 was indicative of a diagnosis of ET with sensitivity of 81.0% and specificity of 88.9%.

To furtherly assess the diagnostic power of visual analysis and the width of lateral SNc subregion in differentiating ET form PD_T, we performed NRI analysis. The NRI value of total visual score (cutoff value at 8) and the width of lateral SNc subregion (cutoff value at 0.525 mm) was 0.794%, and it did not reach the significant statistical difference ($p = 0.457$).

4. Discussion

In our study, we found the neuromelanin of SNc on NM-MRI was significantly reduced in PD_T compared with the ET and controls. On the contrary, SNc neuromelanin did not significantly decrease in ET patients compared with controls. These results suggested the neuromelanin changes of SNc in ET and PD_T follow the different patterns, which were in line with the previous study reported by Reimão et al. [16]. Moreover, we found the neuromelanin of PD_T was more apparently decreased in the lateral and central SNc subregions. This finding may contribute to the mild disease severity with Hoehn and Yahr stage 1–2 for our PD_T patients, and was corresponded to the pathology in PD that SNc dopamine cell loss extended from the ventrolateral to the dorsal region [21]. Some studies indicated that ET had a PD-like neuroimaging features [22], while our results displayed there were no neuromelanin reduction of SNc in ET patients compared with controls. Cortico-olivo-cerebello-thalamo circuit was reported involved in ET [23], which might explain our results.

Complex phenomenology in ET leads to over diagnosis in as many of 30–50% patients [2]. PD_T cases may manifest very minimal or absent bradykinesia. Therefore, the diagnosis only based on clinical symptoms and surface EMG might not be accurate enough, particularly in the early stage or with atypical symptoms and signs. Neuroimaging techniques are potential to lower diagnostic errors. Our results showed the width of lateral SNc subregion as an optimal diagnostic biomarker to distinguish ET from PD_T had an AUC of 0.923, and the diagnostic sensitivity and specificity were only slightly lower than DAT scan [24]. The other NM-MRI parameters in our study including CNR of central subregion and the visual total score showed relatively high diagnostic value as well, and their obtained accuracy was similar to transcranial sonography [25]. Moreover, recent studies investigated that, in PD patients, decreased volume and CNR of substantia nigra on NM-MRI were both positively correlated with the corresponding DAT density detected by SPECT with FP-CIT [26]. Therefore, certain observations in our study suggested that NM-MRI might be a useful tool to diagnose and differentiate tremor disorders without contrast agent.

Visual analysis, which did not need post-processing, such as user-defined ROI or semi-automated measurement, was a flexible and reliable way to evaluate the brain changes, including cortical atrophy [27], as well as the high spot of neuromelanin in locus ceruleus on NM-MRI [28]. The AUC of total visual score to differentiate ET from PD_T was 0.865 in our study, indicating a good diagnostic power. Despite the fact that AUC realized popularity in diagnostic testing, its limitations could not be ignored, including lack of clinical relevance and difficulty in explanation of small-scale changes [20]. NRI could overcome these limitations and quantify how well a new biomarker based on re-classification tables [20]. Using NRI analysis, we found the total visual scores and the width of lateral subregion on NM-MRI showed the same diagnostic ability. Moreover, the total visual scores indicated a high inter-observer consistency. Thus, NM-MRI combining our visual analysis could be a flexible and helpful approach to differentiate ET from PD_T with a high accuracy.

Notably, the patients with ET and PD_T recruited in our study were all drug naïve, which eliminated the undefined confounding factors from medication [29]. However, we also acknowledged several limitations in our study. Firstly, the ET patients we recruited were from a clinical setting, thus restricting our results generalizability to population-dwelling cases. Secondly, considering the relatively small number of patients studied, replication in larger samples was warranted. Thirdly, long acquisition time of NM-MRI sequence might influence subjects' tolerance and bring motion artifact. However, taking proper fixation of head, most NM-MRI images obtained satisfactory quality. Finally, as our study was a case-control study, our results could not indicate the relationship between NM-MRI parameters in SNc and the disease progression. However, a longitudinal study with small sample size reported that the total area and signal intensity of the SNc upon

follow-up NM-MRI were significantly smaller than those on initial NM-MRI in the patients with PD [30]. Therefore, Neuromelanin imaging in the SNc might be a potential biomarker to track disease progression. The longitudinal cohort study was also needed to further clarify the relationship and transition between these two tremor disorders.

In conclusion, the neuromelanin changes of SNc in ET and PD_T follow the different patterns. Both quantitative measurement and visual analysis showed good diagnostic power for the differentiating ET from PD_T subtype on NM-MRI. As the visual analysis was more convenient, NM-MRI combining visual analysis of SNc was a potential diagnostic biomarker in the work-up of tremor disorders.

Financial disclosures/conflict of interest

None.

Funding

This research did not receive any specific grant from funding agencies in the public, commercial, or not-for-profit sectors.

Acknowledgements

The authors thank Prof. Jian Wang (Department of Neurology, Huashan Hospital, Fudan University) for critical reading of the article, and Prof. Naiqing Zhao (School of Public Health, Fudan University) for advice on statistical analyses.

Appendix A. Supplementary data

Supplementary data related to this article can be found at <https://doi.org/10.1016/j.parkreldis.2018.07.007>.

References

- [1] O. Dogu, S. Sevim, H. Camdeviren, T. Sasmaz, R. Bugdayci, M. Aral, H. Kaleagasi, S. Un, E.D. Louis, Prevalence of essential tremor: door-to-door neurologic exams in Mersin Province, Turkey, *Neurology* 61 (12) (2003) 1804–1806.
- [2] E.D. Louis, Twelve clinical pearls to help distinguish essential tremor from other tremors, *Expert Rev. Neurother.* 14 (9) (2014) 1057–1065.
- [3] R. Zimmermann, G. Deuschl, A. Hornig, J. Schulte-Monting, G. Fuchs, C.H. Lucking, Tremors in Parkinson's disease: symptom analysis and rating, *Clin. Neuropharmacol.* 17 (4) (1994) 303–314.
- [4] O. Cohen, S. Pullman, E. Jurewicz, D. Watner, E.D. Louis, Rest tremor in patients with essential tremor: prevalence, clinical correlates, and electrophysiologic characteristics, *Arch. Neurol.* 60 (3) (2003) 405–410.
- [5] S. Jain, S.E. Lo, E.D. Louis, Common misdiagnosis of a common neurological disorder: how are we misdiagnosing essential tremor? *Arch. Neurol.* 63 (8) (2006) 1100–1104.
- [6] J. Benito-Leon, Essential Tremor: a Neurodegenerative Disease? *Tremor Other Hyperkinet Mov (NY)* 4 (2014) 252.
- [7] M.A. Thenganatt, J. Jankovic, The relationship between essential tremor and Parkinson's disease, *Park. Relat. Disord.* 22 (Suppl 1) (2016) S162–S165.
- [8] E.D. Louis, Non-motor symptoms in essential tremor: a review of the current data and state of the field, *Park. Relat. Disord.* 22 (Suppl 1) (2016) S115–S118.
- [9] E.D. Louis, P.L. Faust, J.P. Vonsattel, L.S. Honig, A. Rajput, C.A. Robinson, et al., Neuropathological changes in essential tremor: 33 cases compared with 21 controls, *Brain* 130 (12) (2007) 3297–3307.
- [10] A.H. Rajput, C.A. Robinson, M.L. Rajput, S.L. Robinson, A. Rajput, Essential tremor is not dependent upon cerebellar Purkinje cell loss, *Park. Relat. Disord.* 18 (5) (2012) 626–628.
- [11] H. Stockner, I. Wurster, Transcranial sonography in essential tremor, *Int. Rev. Neurobiol.* 90 (2010) 189–197.
- [12] F. Novellino, A. Cherubini, C. Chiriaco, M. Morelli, M. Salsone, G. Arabia, et al., Brain iron deposition in essential tremor: a quantitative 3-Tesla magnetic resonance imaging study, *Mov. Disord.* 28 (2) (2013) 196–200.
- [13] I.U. Isaias, G. Marotta, S. Hirano, M. Canesi, R. Benti, A. Righini, et al., Imaging essential tremor, *Mov. Disord.* 25 (6) (2010) 679–686.
- [14] L. Zecca, L. Casella, A. Albertini, C. Bellei, F.A. Zucca, M. Engelen, et al., Neuromelanin can protect against iron-mediated oxidative damage in system modeling iron overload of brain aging and Parkinson's disease, *J. Neurochem.* 106 (4) (2008) 1866–1875.
- [15] M. Sasaki, E. Shibata, K. Tohyama, J. Takahashi, K. Otsuka, K. Tsuchiya, et al., Neuromelanin magnetic resonance imaging of locus ceruleus and substantia nigra in Parkinson's disease, *Neuroreport* 17 (11) (2006) 1215–1218.

- [16] S. Reimao, P. Pita Lobo, D. Neutel, L.C. Guedes, M. Coelho, M.M. Rosa, et al., Substantia nigra neuromelanin-MR imaging differentiates essential tremor from Parkinson's disease, *Mov. Disord.* 30 (7) (2015) 953–959.
- [17] G. Deuschl, P. Bain, M. Brin, Consensus statement of the movement disorder society on tremor, *Ad Hoc Scientific committee, Mov. Disord.* 13 (Suppl 3) (1998) 2–23.
- [18] R.B. Postuma, D. Berg, M. Stern, W. Poewe, C.W. Olanow, W. Oertel, et al., MDS clinical diagnostic criteria for Parkinson's disease, *Mov. Disord.* 30 (12) (2015) 1591–1601.
- [19] L. Jin, J. Wang, H. Jin, G. Fei, Y. Zhang, W. Chen, et al., Nigral iron deposition occurs across motor phenotypes of Parkinson's disease, *Eur. J. Neurol.* 19 (7) (2012) 969–976.
- [20] M.J. Pencina, R.B. D'Agostino Sr., R.B. D'Agostino Jr., R.S. Vasan, Evaluating the added predictive ability of a new marker: from area under the ROC curve to reclassification and beyond, *Stat. Med.* 27 (2) (2008) 157–172 discussion 207–212.
- [21] J.M. Fearnley, A.J. Lees, Ageing and Parkinson's disease: substantia nigra regional selectivity, *Brain* 114 (5) (1991) 2283–2301.
- [22] I.U. Isaias, M. Canesi, R. Benti, P. Gerundini, R. Cilia, G. Pezzoli, et al., Striatal dopamine transporter abnormalities in patients with essential tremor, *Nucl. Med. Commun.* 29 (4) (2008) 349–353.
- [23] R.C. Helmich, I. Toni, G. Deuschl, B.R. Bloem, The pathophysiology of essential tremor and Parkinson's tremor, *Curr. Neurol. Neurosci. Rep.* 13 (9) (2013) 378.
- [24] H.T.S. Benamer, J. Patterson, D.G. Grosset, J. Booij, K. de Bruin, E. van Royen, et al., Accurate differentiation of parkinsonism and essential tremor using visual assessment of [(123) I]-FP-CIT SPECT imaging: the [(123) I]-FP-CIT study group, *Mov. Disord.* 15 (3) (2000) 503–510.
- [25] A. Shafieesabet, S.M. Fereshtehnejad, A. Shafieesabet, A. Delbari, H.R. Baradaran, R.B. Postuma, et al., Hyperechogenicity of substantia nigra for differential diagnosis of Parkinson's disease: a meta-analysis, *Park. Relat. Disord.* 42 (2017) 1–11.
- [26] I.U. Isaias, P. Trujillo, P. Summers, G. Marotta, L. Mainardi, G. Pezzoli, L. Zecca, A. Costa, Neuromelanin imaging and dopaminergic loss in Parkinson's disease, *Front. Aging Neurosci.* 8 (2016) 196.
- [27] C. Moller, W.M. van der Flier, A. Versteeg, M.R. Benedictus, M.P. Wattjes, E.L. Koedam, et al., Quantitative regional validation of the visual rating scale for posterior cortical atrophy, *Eur. Radiol.* 24 (2) (2014) 397–404.
- [28] M. Ehrminger, A. Latimier, N. Pyatigorskaya, D. Garcia-Lorenzo, S. Leu-Semenescu, M. Vidailhet, et al., The coeruleus/subcoeruleus complex in idiopathic rapid eye movement sleep behaviour disorder, *Brain* 139 (4) (2016) 1180–1188.
- [29] S. Fahn, D. Oakes, I. Shoulson, K. Kieburtz, A. Rudolph, A. Lang, et al., G. Parkinson Study, Levodopa and the progression of Parkinson's disease, *N. Engl. J. Med.* 351 (24) (2004) 2498–2508.
- [30] K. Matsuura, M. Maeda, K.I. Tabei, M. Umino, H. Kajikawa, M. Satoh, et al., A longitudinal study of neuromelanin-sensitive magnetic resonance imaging in Parkinson's disease, *Neurosci. Lett.* 633 (2016) 112–117.